An olfactory neuron responds stochastically to temperature and modulates *Caenorhabditis elegans* thermotactic behavior

David Biron*†‡, Sara Wasserman*‡, James H. Thomas§, Aravinthan D. T. Samuel†, and Piali Sengupta*¶

*Department of Biology and National Center for Behavioral Genomics, Brandeis University, Waltham, MA 02454; †Department of Physics, Harvard University, Cambridge, MA 02138; and §Department of Genome Sciences, University of Washington, Seattle, WA 98195

Communicated by Eve E. Marder, Brandeis University, Waltham, MA, May 23, 2008 (received for review April 10, 2008)

Caenorhabditis elegans **navigates thermal gradients by using a behavioral strategy that is regulated by a memory of its cultivation temperature (T_c). At temperatures above or around the T_c, animals respond to temperature changes by modulating the rate of stochastic reorientation events. The bilateral AFD neurons have been implicated as thermosensory neurons, but additional thermosensory neurons are also predicted to play a role in regulating thermotactic behaviors. Here, we show that the AWC olfactory neurons respond to temperature. Unlike AFD neurons, which respond to thermal stimuli with continuous, graded calcium signals, AWC neurons exhibit stochastic calcium events whose frequency is stimulus-correlated in a T_c-dependent manner. Animals lacking the AWC neurons or with hyperactive AWC neurons exhibit defects in the regulation of reorientation rate in thermotactic behavior. Our observations suggest that the AFD and AWC neurons encode thermal stimuli via distinct strategies to regulate *C. elegans* thermotactic behavior.**

calcium imaging | G protein-coupled receptor | AWC neuron | isothermal tracking

Many animals navigate their environment by using behavioral strategies that are probabilistic in nature. In the biased random-walk strategy used by *Escherichia coli* and *Caenorhabditis elegans* to navigate chemical gradients, periods of forward movement are interrupted by turns or reversals that reorient the organism (1, 2). The frequency of reorientation events is governed by environmental cues and the animal's past experience, but the occurrence of individual turns and reversals is unpredictable and stochastic (3–6). The mechanisms by which sensory neurons and downstream circuits modulate the probability of reorientation events in complex organisms is not well understood.

C. elegans thermotactic behavior provides an excellent system in which to explore the sensorimotor strategies underlying behavior. The behavior of *C. elegans* on a thermal gradient depends on a memory of its cultivation temperature (T_c) (7). At temperatures (T) that are higher than the T_c ($T>T_c$), animals move down the gradient (cryophilic behavior). Cryophilic behavior is mediated by a biased random-walk strategy such that animals decrease turning frequency when moving down the gradient and increase turning frequency when moving up the gradient (8). At $T\sim T_c$, animals exhibit a distinct behavior called isothermal tracking, where they orient perpendicular to the gradient and follow isotherms by suppressing turns (7). Thus, regulation of turning rate is critical for *C. elegans* thermotactic behavior.

Components of the neuronal circuit underlying thermotactic behaviors in *C. elegans* have been identified (9). The bilateral AFD thermosensory neurons are major thermosensory neurons in the circuit (9). The AFD neurons respond to temperature stimuli only above a threshold temperature corresponding to the T_c, thereby providing a cellular correlate for the T_c memory (10–12). However, the AFD neurons are similarly active in the temperature ranges at which animals exhibit isothermal tracking and cryophilic behavior, suggesting that activity of the AFD neurons cannot account for all aspects of thermotactic behavior (9, 11).

Here, we report that the bilateral AWC olfactory neuron type also responds to temperature. We find that the AWC neurons respond stochastically, but in a stimulus-correlated manner, to thermal stimuli at both $T\geq T_c$ and $T<T_c$. Moreover, the AWC neurons modulate turning frequency on thermal gradients such that thermotactic behaviors are altered in animals lacking, or with hyperactive, AWC neurons. Our results implicate a second sensory neuron type in the modulation of thermotactic behavior and suggest that distinct encoding strategies at the sensory periphery contribute to the generation of spatial navigation behavior.

Results

The AWC Olfactory Neurons Respond Stochastically to Temperature. We focused on the AWC olfactory neurons because these neurons are presynaptic to interneurons previously implicated in the thermosensory circuit (9, 13). To monitor intracellular calcium (Ca^{2+}) levels in response to thermal stimuli, we expressed the genetically encoded Ca^{2+} sensor G-CaMP (14) in the AWC neurons by using the *str-2* promoter. This promoter drives expression in either the left or the right AWC neuron (*str-2*^{ON} neuron; the non-*str-2*-expressing neuron is referred to as the *str-2*^{OFF} neuron) (15). Animals were grown at a defined temperature in the presence of food (T_c), and Ca^{2+} dynamics were examined in the absence of food. The AWC neurons are depolarized upon food removal, reflected in a large transient increase in intracellular Ca^{2+} levels with a half-life of 20 s (3). To separate the effects of food removal from measured temperature responses, we performed all measurements 10 min after removal of animals from food.

We first examined Ca^{2+} dynamics in the AWC neurons of animals in the absence of a stimulus. We observed rare Ca^{2+} events in the AWC neuronal soma in approximately one-third of imaged animals (Fig. 1*A*); the remaining neurons did not show any events and were not followed further. These events were characterized by two time scales: a rapid 2- to 3-s rise in the concentration of intracellular Ca^{2+} followed by a 10- to 15-s decay to baseline (Fig. 1*A*). The timing of individual events appeared to be stochastic and could not be reliably predicted

Author contributions: D.B., S.W., A.D.T.S., and P.S. designed research; D.B. and S.W. performed research; D.B., S.W., and J.H.T. contributed new reagents/analytic tools; D.B., S.W., and P.S. analyzed data; and D.B., S.W., and P.S. wrote the paper.

The authors declare no conflict of interest.

‡D.B. and S.W. contributed equally to this work.

¶To whom correspondence should be addressed. E-mail: sengupta@brandeis.edu.

This article contains supporting information online at www.pnas.org/cgi/content/full/0805004105/DCSupplemental.

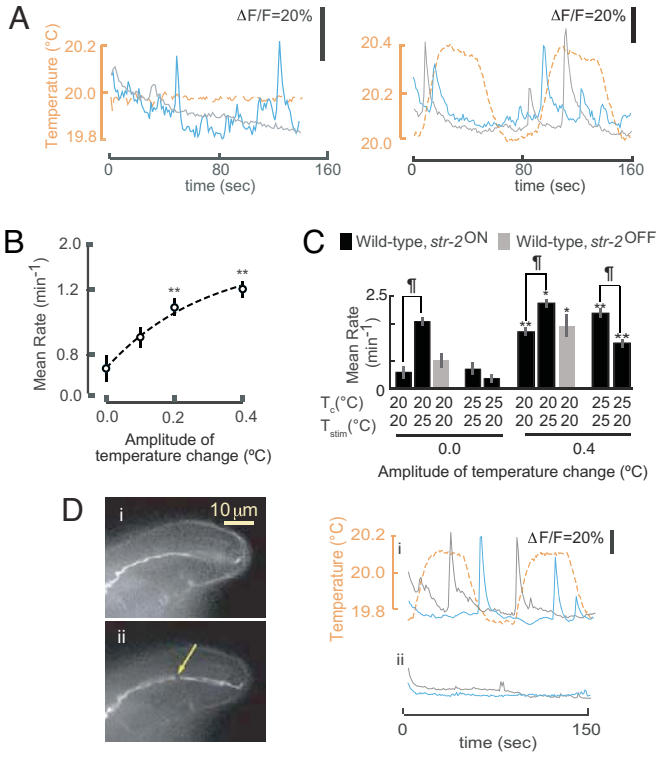

Fig. 1. AWC neurons respond stochastically to temperature. (*A*) Representative examples of Ca^{2+} events of two *str-2*^{ON} AWC neurons (solid lines) expressing G-CaMP. The temperature is indicated by a dashed orange line. T_c = 20°C. (*B*) Average event rate of wild-type *str-2*^{ON} AWC neurons to thermal stimuli of varying amplitudes. **, Rates that are different at $P < 0.01$ and $P < 0.05$, respectively, from the rate in the absence of a varying stimulus. Error bars are ±1 SEM. n = 10–12 neurons each. (*C*) Average event rates in AWC neurons of animals grown at the indicated T_c and examined at the indicated temperature (T_{stim}). ¶, Rates that are different at $P < 0.01$; ** and *, rates that are different at $P < 0.01$ and $P < 0.05$, respectively, from the rate in the absence of a varying stimulus. Error bars are ±1 SEM. n = 10–12 neurons each. (*D*) (*Left*) *str-2*^{ON} AWC dendrite before (*i*) and after (*ii*) femtosecond laser-mediated severing. Arrow indicates the site of severing. (*Right*) Events (solid lines) from the soma of two AWC neurons before (*i*) and after (*ii*) surgery to thermal stimuli (dashed line). T_c = 20°C. Only neurons that showed events before surgery were included in this analysis.

from neuron to neuron or in multiple trials from the same neuron. We determined whether similar events were observed in the AWB olfactory neurons, which are also presynaptic to neurons implicated in the thermosensory circuit (13). However, no changes in intracellular Ca^{2+} dynamics were observed in AWB neurons expressing G-CaMP (data not shown), indicating that the observed events in the AWC neurons were likely not the result of movement artifacts.

C. elegans thermotactic behavior requires that animals sense and respond to temperature differences in the range of 0.01–0.5°C, on time scales of ≈2–20 s (8, 11). To characterize temperature events to physiologically relevant stimuli, we next subjected animals to a square wave temperature stimulus with an amplitude of 0.4°C over 15 s around their T_c ($T \sim T_c$). We again observed Ca^{2+} events with rise and decay time scales similar to those of events seen in the absence of an applied thermal stimulus in both *str-2*^{ON} and *str-2*^{OFF} neurons (Fig. 1*A* and data not shown). Individual Ca^{2+} events were stochastically dispersed during the measurement (Fig. 1*A*). Although event rates were low when the temperature was not varied, event rates increased monotonically with increasing stimulus amplitude (Fig. 1 *B* and *C*). Ca^{2+} events were again observed in approximately one-third of the imaged neurons. Although the reasons for observing Ca^{2+} responses in a subset of imaged neurons are unclear, these observations suggest that the AWC neurons respond to thermal stimuli and are responsive to the magnitude of the stimulus.

The AWC Sensory Endings Are Required for Their Temperature Responses. The observed Ca^{2+} events in the AWC neuronal soma could arise as a consequence of inputs or feedback from other neurons or because of intrinsic thermoresponsive properties. Primary sensory signal transduction events are thought to occur at the distal sensory endings of the AWC dendrites (13). We decoupled the AWC sensory endings from their soma by severing the AWC dendrites using a tightly focused femtosecond laser and quantified Ca^{2+} events in the soma before and after surgery (16). We found that stimulated events in the AWC soma were abolished upon surgery (Fig. 1*D*), whereas sham-operated animals continued to exhibit events (10 of 12 sham-operated and 0 of 8 operated animals retained events after surgery). This result indicates that the sensory endings of the AWC neurons were essential for their temperature-regulated stochastic responses, suggesting that the AWC neurons may directly respond to thermal stimuli. These experiments further indicate that the observed Ca^{2+} events were likely not caused by motion artifacts during imaging.

The AWC Neurons Are Responsive to Temperature Changes at both $T > T_c$ and $T < T_c$. The AFD neurons are responsive to temperature changes only at $T \geq T_c$ (11, 12). We next determined whether the AWC neurons respond to temperature changes at $T > T_c$ and $T < T_c$. We grew animals at 20°C or 25°C (T_c) and examined AWC neuronal responses upon shifting animals to 25°C or 20°C (T_{stim} is stimulation temperature), respectively (Fig. 1*C*). Event rates were significantly increased in animals grown at T_c = 20°C and examined without or with a varying thermal stimulus ≈25°C, compared with rates in animals grown and examined at 20°C (Fig. 1*C*). Conversely, the event rates of animals grown at 25°C and examined at 20°C were decreased, compared with animals grown and examined at 25°C (Fig. 1*C*). However, overall event rates increased in response to a varying thermal stimulus under all conditions (Fig. 1*C*). These results indicate that event rates in the AWC neurons are modulated when animals are shifted to a new temperature from their T_c. Moreover, unlike the AFD neurons, the AWC neurons are responsive to varying thermal stimuli when shifted to temperatures both above and below their T_c.

The Responses of the AWC Neurons Are Stimulus-Correlated in a T_c-Dependent Manner. We next investigated whether the stochastic temperature events observed in the AWC neurons were correlated with the stimulus in a T_c-dependent manner. We subjected animals to a square wave temperature stimulus at $T > T_c$ and $T < T_c$, and quantified the average change in fluorescence in the AWC neurons as a function of time.

We found that although the occurrence of an individual event in the AWC soma was not time-locked to the stimulus, the average response revealed a correlation with the stimulus at both above and below the T_c (Fig. 2). At $T \geq T_c$, the average Ca^{2+} response in the AWC neurons increased during the rising phase of the stimulus and decreased rapidly after stimulus plateau [Fig. 2 *A* and *B* and supporting information (SI) Fig. S1*A*]. However, when subjected to a similar square wave stimulus at $T < T_c$, the average Ca^{2+} response increased only after an ≈20-s delay after the temperature rise (Fig. 2*C*). This delay was not specific to the T_c and experimental temperature because a similar delay was observed in animals grown at 22.5°C and subjected to a temperature stimulus with a longer period centered ≈18°C (Fig. 2*D*). The observed changes in average responses were caused by differences in event rates, and not sizes of Ca^{2+} events at

NEUROSCIENCE

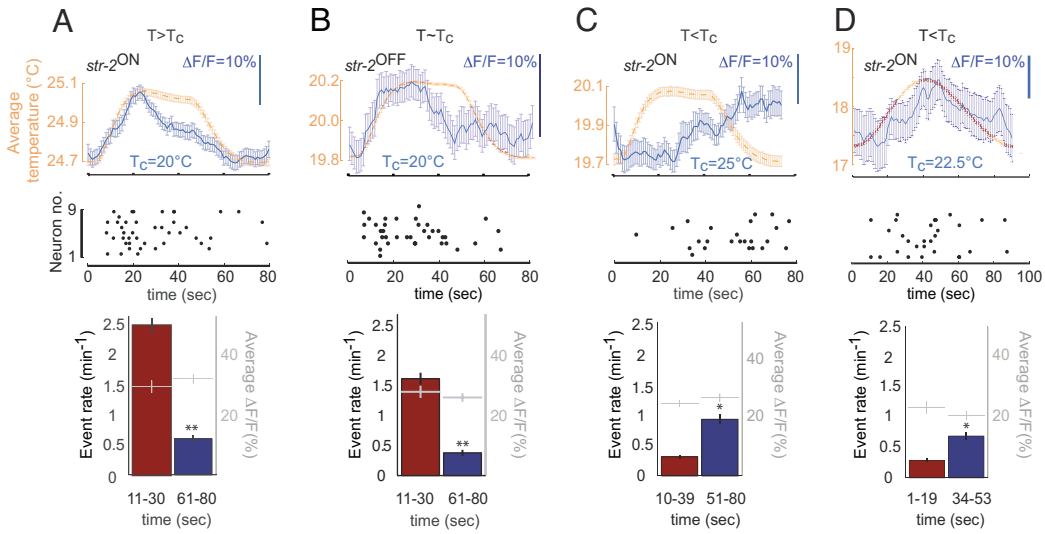

Fig. 2. Temperature responses in the AWC neurons are stochastic but stimulus-correlated. (*A–D*) Responses of AWC neurons to temperature stimuli (dashed orange lines, *Top*) are shown as raster plots of neurons (*Middle*), where each dot represents a event. The average responses (blue solid line, *Top*) were obtained by summing the responses of 8–10 neurons (see *Materials and Methods*). The magnitude of the difference in average response between any two time points is indicated by the scale bars. To demonstrate the correlation between the stimulus and the response graphically, the summed response curves were scaled to the size of the stimulus. Error bars are ±1 SEM. (*Bottom*) Average event rates and amplitudes for the indicated time periods during the stimulation. ** and *, $P < 0.01$ and 0.05, respectively.

different phases of the stimulus (Fig. 2 *A–D*). Thus, responses in the AWC neurons are stochastic but stimulus-correlated with different dynamics at both $T \geq T_c$ and $T < T_c$. The observed average AWC responses may be considered analogous to the macroscopic sodium currents measured in voltage clamp experiments, which are stimulus-correlated when summed across multiple trials but arise because of the stochastic opening and closing of single sodium channels (17).

The AWC Neurons Are Hyperactive in *srtx-1* G Protein-Coupled Receptor (GPCR) Mutants. To understand better the role of AWC neurons in the thermosensory circuit, we wished to identify mutants with altered AWC thermoresponsive properties. We previously identified the *srtx-1* (serpentine receptor class tx; previously referred to as *B0496.5*) GPCR gene and showed that the SRTX-1 protein is expressed in and localized specifically to the sensory endings of the AFD and AWC neurons (18). SRTX-1 belongs to a GPCR subfamily that is highly conserved in *Caenorhabditis* species but is absent in other organisms (Fig. S2 *A* and *B*). Given its restricted expression pattern in two temperature-responsive neurons, we examined the role of this molecule in modulating AFD and AWC neuronal functions.

We found that the AWC neurons of *srtx-1*(*tm2064*) and *srtx-1*(*nj62*) (gift from I. Mori, Nagoya University, Nagoya, Japan; Fig. S2*C*) mutants exhibited a markedly high rate of Ca^{2+} events even under nonstimulated conditions (Fig. 3 *A–C*). Similar to wild-type animals, only approximately one-third of imaged AWC neurons in *srtx-1* mutants exhibited Ca^{2+} events. The rate of events was not altered upon increasing the stimulus amplitude in *srtx-1* mutants (Fig. 3 *A–C*). Nevertheless, the responses in the AWC neurons of *srtx-1* mutants retained stimulus-correlation in a T_c-dependent manner (Fig. 3 *D* and *E* and Fig. S1 *B* and *C*). The differences in average responses of *srtx-1* mutants at different phases of the stimulus could again be attributed largely to changes in the rates, and not sizes, of Ca^{2+} events (Fig. 3 *D* and *E*). Ca^{2+} responses in the AFD neurons appeared to be unaffected in *srtx-1* mutants (data not shown). These results suggest that SRTX-1 decreases basal event rate in the AWC neurons.

The AWC Neurons Modulate Cryophilic Behavior at $T > T_c$. We next determined whether the AWC neurons modulate thermotactic navigation behaviors. The AWC neurons have been suggested to promote turning behavior upon food removal (refs. 3, 4, 19, and 20 and Fig. S3). Turning rates are maximal in a ≈15-min period immediately after food removal and decrease thereafter (4, 19) (Fig. S3). To ensure that events caused by food removal contribute minimally to temperature-regulated changes in turning frequency, we conducted all behavioral assays 10 min after food removal and examined the events over the subsequent 30–50 min.

To identify defects, if any, in thermotactic navigational strategies, we quantified the duration of forward movement in response to temperature changes at $T > T_c$ or $T < T_c$ and computed the cryophilic bias index (21). The cryophilic bias index is defined as [(average duration of forward movement down the gradient) − (average duration of forward movement up the gradient)/(total duration of forward movement)]. Thus, a positive cryophilic bias drives animals down the gradient (cryophilic behavior), zero bias results in random movement (atactic behavior), and a negative cryophilic bias drives animals up the gradient (thermophilic behavior).

At $T > T_c$, mock-ablated animals exhibited a longer duration of forward movement down the gradient, resulting in a positive cryophilic bias index (Fig. 4 *A* and *B* and Fig. S4). AWC-ablated animals exhibited an overall longer duration of forward movement while navigating both up and down the gradient (Fig. 4*A* and Fig. S4). However, the relative increase in forward movement duration when navigating up the gradient was larger than when navigating down the gradient, resulting in a significantly lower cryophilic bias index than that of mock-ablated animals (Fig. 4*B*). This result suggests that AWC regulates turning frequency in a temperature-regulated manner and modulates cryophilic navigation behavior. At $T < T_c$, AWC-ablated animals also exhibited an increased duration of forward movement when navigating both up and down the gradient (Fig. 4*A* and Fig. S4). However, the cryophilic bias indices of AWC-ablated or mock-ablated animals were not significantly different from zero, indicating that ablation of the AWC neurons did not affect atactic behavior at $T < T_c$ (Fig. 4*B*).

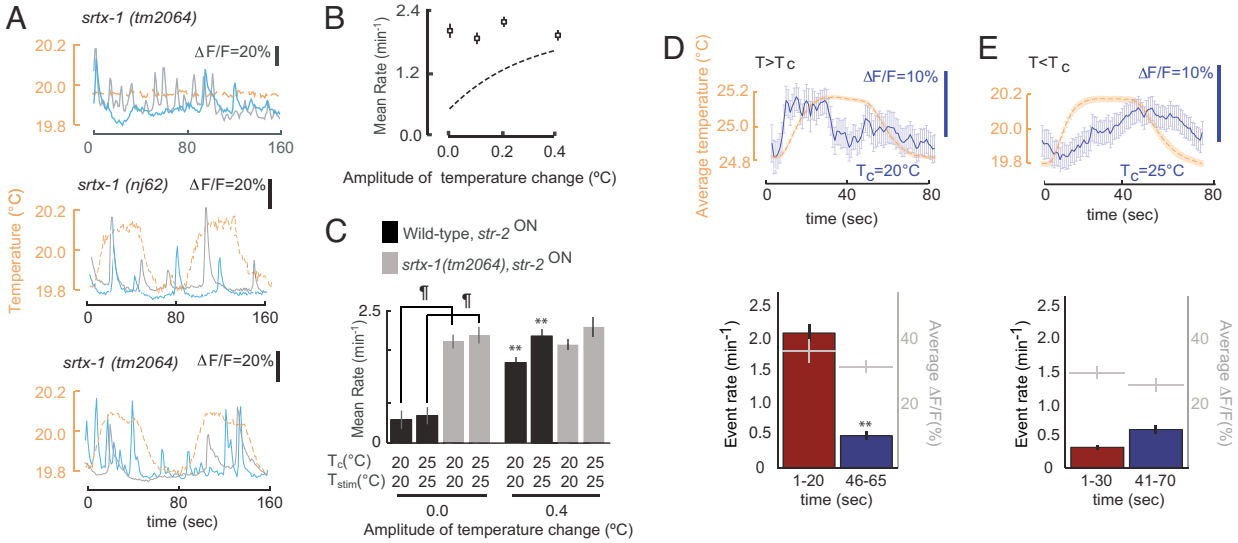

Fig. 3. AWC neurons are hyperactive in *srtx-1* GPCR mutants. (*A*) Events in two *str-2*^{ON} AWC neurons (solid lines) from *srtx-1* mutants. The temperature is indicated by the dashed line. (*B*) Average event rates of *str-2*^{ON} neurons of *srtx-1*(*tm2064*) mutants to thermal stimuli of varying amplitudes. The dashed line shows corresponding data for wild-type *str-2*^{ON} neurons from Fig. 1*B*. (*C*) Average event rates in AWC neurons of wild-type or *srtx-1*(*tm2064*) animals grown at the indicated T_c and examined at the indicated temperature (T_{stim}). ¶, Rates that are different at $P < 0.01$; **, rates that are different at $P < 0.01$ from the rate in the absence of a varying stimulus. Error bars are ±1 SEM. $n = 10–12$ neurons for each. (*D* and *E*) (*Upper*) Average response of *srtx-1*(*tm2064*) animals to a thermal stimulus at $T>T_c$ (*D*) and $T<T_c$ (*E*), obtained by summing responses as in Fig. 2. (*Lower*) Average event rates and amplitudes for the indicated time periods. Error bars are ±1 SEM. $n = 10–12$ AWC neurons. **, $P < 0.01$.

To examine further the role of the AWC neurons in regulating turning frequency, we examined thermotactic navigation behaviors of *srtx-1* mutants. Hyperactivation of the AWC neurons in *srtx-1* mutant is predicted to be associated with an increased turning frequency. We first confirmed this hypothesis by examining the behaviors of *srtx-1* mutants in the presence and absence of food. We found that *srtx-1*(*tm2064*) mutants exhibited a higher turning frequency than wild-type animals even in the presence of food (Fig. S3). This turning rate was further increased upon food removal and sustained for a longer time period (Fig. S3). The altered turning rate phenotype was partly suppressed upon expression of wild-type *srtx-1* in the AWC neurons (Fig. S3), indicating that SRTX-1 acts in the AWC neurons to regulate turning rate.

We found that *srtx-1* mutants also exhibited an increased turning frequency on a linear thermal gradient, reflected in decreased duration of forward movement both up and down the gradient at $T>T_c$ (Fig. 4*A* and Fig. S5). However, the cryophilic bias index of *srtx-1* mutants was not significantly different from those of wild-type animals (Fig. 4*B*). Thus, increasing the basal event rate in the AWC neurons increased turning frequency but did not significantly affect thermotactic navigation behavior under the examined conditions.

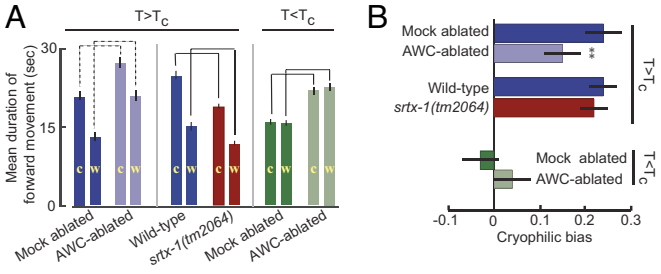

Fig. 4. AWC neurons regulate thermotactic navigation behavior. (*A*) Mean duration of forward movement as a function of direction on a temperature gradient at $T>T_c$ or $T<T_c$. $T_c = 15$°C. Movement toward the colder and warmer directions is indicated by c and w, respectively. Histograms of forward movement duration are shown in Figs. S4 and S5. Gradient steepness was 0.5°C cm^{-1}. Mean movement duration was calculated from five to seven independent plates and >40 animals for every condition. Solid and dashed brackets compare values that are different at $P < 0.01$ and $P < 0.05$, respectively. Error bars are ±1 SEM. The average velocity of movement of mock-ablated and AWC-ablated animals was 0.23 ± 0.08 mm s^{-1} and 0.27 ± 0.09 mm s^{-1} at $T>T_c$, and 0.22 ± 0.08 mm s^{-1} and 0.26 ± 0.09 mm s^{-1} at $T<T_c$. The average velocity of movement of wild-type and *srtx-1*(*tm2064*) animals was 0.30 ± 0.07 mm s^{-1} and 0.29 ± 0.07 mm s^{-1}, respectively. (*B*) Cryophilic bias indices at $T>T_c$ or $T<T_c$. The cryophilic bias index is defined in the text (32) and was calculated from data in *A*. **, $P < 0.01$. Cryophilic bias indices at $T<T_c$ were not significantly different from zero. All mock-ablated and AWC-ablated strains contain the *che-1*(*p674*) mutation (33) and stably integrated copies of the *ceh-36*p::*gfp* fusion gene (34).

Suppression of AWC Neuronal Event Rate Is Essential for Isothermal Tracking Behavior. Because the AWC neurons modulate turning frequency, we next examined the role of the AWC neurons in isothermal tracking behavior. Animals must sense temperature differences of ≈0.01°C s^{-1} on a 1°C per cm gradient to maintain trajectory on an isothermal track (22). Although we are unable to reproduce this stimulus for imaged neurons because of technical limitations, we noted that the AWC neurons exhibited low stochastic event rates below 0.1°C changes in 15 s at $T \sim T_c$ (Fig. 1 *B* and *C*), suggesting that the AWC neurons are relatively inactive during isothermal tracking behavior.

Because the duration of individual isothermal tracks is regulated by turning frequency, we first compared average track duration of wild-type, AWC-ablated, and *srtx-1* mutant animals. We found that ablation of both AWC neurons resulted in a minor, but significant increase in average track duration (Fig. 5*A* and Fig. S6). However, the track duration of *srtx-1* mutant animals was significantly decreased (Fig. 5*A*). This behavioral defect was fully rescued by ablating the AWC neurons (Fig. 5*A*), suggesting that hyperactivation of the AWC neurons contributes to the defective tracking behavior of *srtx-1* mutants. AWC-ablated and *srtx-1* mutant animals initiated tracking within the same temperature range as wild-type animals (data not shown),

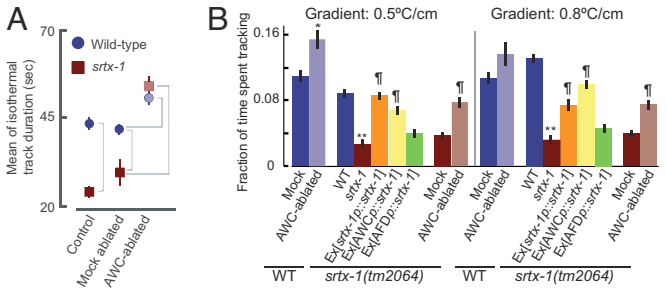

Fig. 5. The AWC neurons regulate isothermal tracking behavior. (*A*) Mean duration of all isothermal tracks on a 0.5°C per cm gradient. T_c = 20°C. Histograms of all track durations are shown in Fig. S6. Brackets compare values that are different at $P < 0.01$. Mock-ablated and AWC-ablated animals contain the *che-1*(*p674*) allele and integrated copies of the *ceh-36*p::*gfp* fusion gene. The *srtx-1*(*tm2064*) allele was used. n = 5–7 assays (12–20 animals per assay) for each condition. Error bars are ±1 SEM. (*B*) Fraction of total time spent performing isothermal tracking behavior on gradients of indicated steepness. The *srtx-1*(*tm2064*) allele was used; behaviors of *srtx-1*(*nj62*) mutants are shown in Fig. S7. Wild-type *srtx-1* was expressed in the AFD neurons under the *gcy-8* promoter, the AWC and ASE neurons under the *ceh-36* promoter, and in both the AFD and AWC neurons under its own promoter. Average events of two independent transgenic lines are shown for each construct; the behaviors of each line were similar. T_c = 20°C. n = 5–7 assays (12–20 animals per assay) for each condition. Error bars are ±1 SEM. ** and *, values that are different from the corresponding wild-type values at $P < 0.01$ and $P < 0.05$, respectively; ¶, values different from the corresponding *srtx-1*(*tm2064*) values at $P < 0.01$.

indicating that the AWC neurons do not affect the selection of the temperature range in which tracking behavior is exhibited.

As a second measure of isothermal tracking behavior, we also quantified the fraction of time an animal spends tracking isotherms by summing the duration of all isothermal tracks exhibited by a population of animals on gradients of different steepness in a defined time period (see *SI Materials and Methods*) (22). Consistent with increased track duration, AWC-ablated animals spent a larger fraction of time tracking isotherms than mock-ablated animals (Fig. 5*B*). Conversely, *srtx-1* mutants spent a significantly shorter fraction of time tracking isotherms (Fig. 5*B* and Fig. S7). This defect in isothermal tracking behavior could be rescued by ablating the AWC neurons in *srtx-1* mutants (Fig. 5*B*) or by expressing *srtx-1* specifically in the AWC, but not in the AFD neurons (Fig. 5*B*). Similar defects were observed in animals carrying two additional alleles of *srtx-1* (Fig. S7; gift from I. Mori). Taken together, these observations suggest that effective execution of isothermal tracking behavior requires suppression of AWC neuronal activity.

Discussion

We have shown that the AWC olfactory neurons are responsive to temperature and contribute to the precise execution of thermosensory behaviors. The timing of individual Ca^{2+} events in the AWC neurons in response to a time-varying thermal stimulus is unpredictable throughout the measured time period, although it is correlated with the stimulus. The mechanisms underlying the generation of the stochastic events in the AWC neurons are not yet clear. The ciliated sensory endings of the AWC neurons are required for the temperature-induced responses, implying that these neurons are directly responsive to thermal stimuli and that stochasticity in event occurrence may be an intrinsic neuronal property. Consistent with this notion, we find that loss of function of the cilia-localized SRTX-1 GPCR hyperactivates the AWC neurons, suggesting that SRTX-1 acts in the AWC cilia to dampen neuronal activity. The timing and rate of observed events in the AWC neurons may be modulated by intrinsic neuronal oscillatory mechanisms together with stimulus noise and/or by neuromodulation via feedback-mediated inputs from other circuit components (23–27).

Activity of both the AFD and the AWC neurons is essential for the execution of thermotactic behaviors with high fidelity and precision. At $T > T_c$, the overall event rate in the AWC neurons is high, and both the AFD and AWC neurons exhibit increased activity as temperatures rise (refs. 11 and 12 and this report). It has been reported that ablation of the AFD neurons weakens but does not abolish cryophilic behavior (9, 16), and we find that ablation of the AWC neurons also weakens cryophilic behavior. Thus, the AFD and AWC neurons may act in concert to increase turning rate when animals move up the gradient at $T > T_c$. We note that stochastic AWC events and turn occurrence upon thermal stimulation happen on relatively similar time scales, suggesting that a single AWC event may be sufficient to trigger a turn under specific conditions. However, it is likely that additional neuron(s) contribute to temperature-regulated modulation of movement.

At $T < T_c$, AWC neuronal events do not appear to modulate turning rate. Activity of the AWC neurons in the absence of AFD neuronal activity may not be sufficient to trigger a turn in our experimental conditions. However, *C. elegans* has been reported to move up the gradient at $T < T_c$ under certain conditions (7, 9, 28), although this thermophilic behavior occurs at a slower rate than cryophilic behavior (29). It is intriguing to note that the 20-s delay in the event rate rise to increasing temperatures at $T < T_c$ equals the average forward movement duration of animals in an isotropic environment (8). The consequent predicted delay in a reorientiation event could thus allow animals to move up a gradient. Taken together with the markedly lower overall event rate in the AWC neurons at $T < T_c$ compared with the rate at $T > T_c$, our results provide a plausible explanation for the weak thermophilic behavior observed only under defined conditions at $T < T_c$ (29).

The AWC neurons also play a critical role in modulating isothermal tracking behavior at $T \sim T_c$. Our experiments suggest that the AWC neurons are relatively inactive under conditions of small temporal temperature changes close to the T_c. This suppression of AWC neuronal events may be essential for isothermal tracking via suppression of turning frequency. Consistent with this hypothesis, we find that *srtx-1* mutants exhibit poor isothermal tracking behavior because of a high basal rate of AWC neuronal events. It has been shown that animals do not actively pursue isothermal alignment, but once serendipitously aligned along an isotherm at $T \sim T_c$, they track isotherms by suppressing turns (22). We suggest that activity of the AFD neurons, together with inactivity of the AWC neurons when tracking an isotherm, allows animals to perform isothermal tracking behavior. Thus, although the AFD neurons respond similarly to temperature changes at $T \geq T_c$, the distinct responses of the AWC neurons at $T \sim T_c$ and $T > T_c$ may allow the animal to exhibit distinct behaviors in different temperature ranges.

The role of AWC in thermosensation and regulation of thermotactic behaviors has recently been described in an independent study (30). However, the AWC neurons were reported to respond deterministically to thermal stimuli only at $T > T_c$ in this work, similar to the responses of the AFD neurons. Moreover, hyperactivation of the AWC neurons was shown to modulate cryophilic behavior, although isothermal tracking behavior was not examined. These discrepancies may be caused by the use of large temperature steps (3–9°C), as opposed to the 0.1–0.4°C amplitude temperature steps used in this work, and differences in behavioral assays and measurements.

A goal of behavioral neuroscience is to identify and define the mechanisms by which sensory information is encoded and processed to generate specific behaviors. The compact size and known anatomical connectivities of the *C. elegans* nervous system provide an excellent system in which to achieve this goal.

Indeed, theoretical modeling based on known neuronal and circuit functions has defined circuit motifs capable of performing spatial navigation behaviors in response to chemical or thermal stimuli (5, 6). These motifs generally rely on the assumption that *C. elegans* sensory neurons and interneurons form a graded processing network based on the apparent absence of action potentials in *C. elegans* neurons (31). Our finding that the AWC neurons exhibit stochastic but stimulus-correlated responses suggests that alternative models for sensorimotor computations must also be considered. It will be particularly interesting to determine how the signals from the AFD and AWC neuron types are weighted as information is processed through the circuit. We expect that the combination of theoretical, experimental, and behavioral approaches possible in *C. elegans* will further define how neurons encode and translate sensory information into precise behavioral outcomes.

Materials and Methods

Strains. *srtx-1*(*tm2064*) was obtained from the National Bioresource Project (Japan) and outcrossed four times before analysis. *srtx-1*(*nj62*) and *srtx-1*(*nj63*) were outcrossed 11 and 10 times, respectively (gift from I. Mori).

Molecular Biology. Expression constructs were generated by subcloning *srtx-1* genomic sequences downstream from the gene-specific promoters in a *C. elegans* expression vector (gift from A. Fire, Stanford University, Stanford, CA). Constructs and amplified sequences were confirmed by sequencing.

Behavioral Assays. Young adult animals grown overnight at a specific temperature were transferred to a 9-cm-diameter plate with a linear spatial thermal gradient without food. After equilibration for 10 min, worm positions and trajectories over time and isothermal track position and duration were recorded and quantified as described (21, 32) and in *SI Materials and Methods*.

Calcium Imaging. Calcium imaging was performed essentially as described (10, 11). Imaging was performed by using wild-type and *srtx-1* mutant strains carrying the same *str-2*p::G-CaMP-containing extrachromosomal array (gift from C. Bargmann, The Rockefeller University, New York) (3). The presence of this array did not affect thermotactic behaviors of wild-type or *srtx-1* mutant animals (data not shown). On average, two-thirds of the worms did not exhibit a event and were excluded from the analysis. The number of nonresponding animals was constant across conditions and genotypes. A detailed description of calcium imaging methods is provided in *SI Materials and Methods*.

Laser Surgery. Laser microsurgery of dendrites and neuronal cell body ablations were performed as described in ref. 17. AWC neurons were identified by the expression of *ceh-36*p::*gfp*, which drives expression in the AWC and ASE neurons (33). To permit visualization of only the AWC neurons, these strains also carried the *che-1*(*p674*) allele, which abolishes *ceh-36*p::*gfp* expression in the ASE neurons (34). Additional details are in *SI Materials and Methods*.

Statistical Analyses. Comparisons were performed by using one-way ANOVA. For multiple comparisons, significant differences were further analyzed by using the post hoc Bonferroni–Dunn test. $P < 0.05$ was considered significant.

ACKNOWLEDGMENTS. We thank H. Sasakura and I. Mori (Nagoya University, Nagoya, Japan) for providing the *nj62* and *nj63* alleles; and S. Chalasani (The Rockefeller University, New York), C. Bargmann, the *Caenorhabditis* Genetics Center, and S. Mitani (National Bioresource Project) for strains. We thank I. Mori for sharing data before publication, and P. Garrity and the Sengupta laboratory for discussion. This work was supported by a Human Frontiers Science Program cross-disciplinary fellowship (to D.B.), the National Science Foundation (to A.D.T.S.), the Sloan and McKnight Foundations (to A.D.T.S.), and the National Institutes of Health (to P.S. and S.W.).

1. Berg HC, Brown DA (1972) Chemotaxis in *E. coli* analysed by three-dimensional tracking. *Nature* 239:500–504.
2. Pierce-Shimomura JT, Morse TM, Lockery SR (1999) The fundamental role of pirouettes in *Caenorhabditis elegans* chemotaxis. *J Neurosci* 19:9557–9569.
3. Chalasani SH, *et al*. (2007) Dissecting a neural circuit for food-seeking behavior in *Caenorhabditis elegans*. *Nature* 450:63–70.
4. Gray JM, Hill JJ, Bargmann CI (2005) A circuit for navigation in *Caenorhabditis elegans*. *Proc Natl Acad Sci USA* 102:3184–3191.
5. Dunn NA, Lockery SR, Pierce-Shimomura JT, Conery JS (2004) A neural network model of chemotaxis predicts functions of synaptic connections in the nematode *Caenorhabditis elegans*. *J Comput Neurosci* 17:137–147.
6. Dunn NA, Conery JS, Lockery SR (2007) Circuit motifs for spatial orientation behaviors identified by neural network optimization. *J Neurophysiol* 98:888–897.
7. Hedgecock EM, Russell RL (1975) Normal and mutant thermotaxis in the nematode *Caenorhabditis elegans*. *Proc Natl Acad Sci USA* 72:4061–4065.
8. Ryu WS, Samuel AD (2002) Thermotaxis in *Caenorhabditis elegans* analyzed by measuring responses to defined thermal stimuli. *J Neurosci* 22:5727–5733.
9. Mori I, Ohshima Y (1995) Neural regulation of thermotaxis in *Caenorhabditis elegans*. *Nature* 376:344–348.
10. Biron D, *et al*. (2006) A diacylglycerol kinase modulates long-term thermotactic behavioral plasticity in *C. elegans*. *Nat Neurosci* 9:1499–1505.
11. Clark DA, Biron D, Sengupta P, Samuel ADT (2006) The AFD sensory neurons encode multiple functions underlying thermotactic behavior in *C. elegans*. *J Neurosci* 26:7444–7451.
12. Kimura KD, Miyawaki A, Matsumoto K, Mori I (2004) The *C. elegans* thermosensory neuron AFD responds to warming. *Curr Biol* 14:1291–1295.
13. White JG, Southgate E, Thomson JN, Brenner S (1986) The structure of the nervous system of the nematode *Caenorhabditis elegans*. *Philos Trans R Soc London Ser B* 314:1–340.
14. Nakai J, Ohkura M, Imoto K (2001) A high signal-to-noise Ca^{2+} probe composed of a single green fluorescent protein. *Nat Biotechnol* 19:137–141.
15. Troemel ER, Sagasti A, Bargmann CI (1999) Lateral signaling mediated by axon contact and calcium entry regulates asymmetric odorant receptor expression in *C. elegans*. *Cell* 99:387–398.
16. Chung SH, Clark DA, Gabel CV, Mazur E, Samuel AD (2006) The role of the AFD neuron in *C. elegans* thermotaxis analyzed using femtosecond laser ablation. *BMC Neurosci* 7:30.
17. Sigworth FJ, Neher E (1980) Single Na^+ channel currents observed in cultured rat muscle cells. *Nature* 287:447–449.
18. Colosimo ME, *et al*. (2004) Identification of thermosensory and olfactory neuron-specific genes via expression profiling of single neuron types. *Curr Biol* 14:2245–2251.
19. Wakabayashi T, Kitagawa I, Shingai R (2004) Neurons regulating the duration of forward locomotion in *Caenorhabditis elegans*. *Neurosci Res* 50:103–111.
20. Tsalik EL, Hobert O (2003) Functional mapping of neurons that control locomotory behavior in *Caenorhabditis elegans*. *J Neurobiol* 56:178–197.
21. Chi CA, *et al*. (2007) Temperature and food mediate long-term thermotactic behavioral plasticity by association-independent mechanisms in *C. elegans*. *J Exp Biol* 210:4043–4052.
22. Luo L, Clark DA, Biron D, Mahadevan L, Samuel AD (2006) Sensorimotor control during isothermal tracking in *Caenorhabditis elegans*. *J Exp Biol* 209:4652–4662.
23. Douglass JK, Wilkens L, Pantazelou E, Moss F (1993) Noise enhancement of information transfer in crayfish mechanoreceptors by stochastic resonance. *Nature* 365:337–340.
24. Braun HA, Wissing H, Schafer K, Hirsch MC (1994) Oscillation and noise determine signal transduction in shark multimodal sensory cells. *Nature* 367:270–273.
25. Braun HA, Bade H, Hensel H (1980) Static and dynamic discharge patterns of bursting cold fibers related to hypothetical receptor mechanisms. *Pflügers Arch* 386:1–9.
26. Schneidman E, Freedman B, Segev I (1998) Ion channel stochasticity may be critical in determining the reliability and precision of spike timing. *Neural Comput* 10:1679–1703.
27. Billimoria CP, DiCaprio RA, Birmingham JT, Abbott LF, Marder E (2006) Neuromodulation of spike-timing precision in sensory neurons. *J Neurosci* 26:5910–5919.
28. Zariwala HA, Miller AC, Faumont S, Lockery SR (2003) Step response analysis of thermotaxis in *Caenorhabditis elegans*. *J Neurosci* 23:4369–4377.
29. Ito H, Inada H, Mori I (2006) Quantitative analysis of thermotaxis in the nematode *Caenorhabditis elegans*. *J Neurosci Methods* 154:45–52.
30. Kuhara A, *et al*. (2008) Temperature sensing by an olfactory neuron in a circuit controlling behavior of *C. elegans*. *Science* 320:803–807.
31. Goodman MB, Hall DH, Avery L, Lockery SR (1998) Active currents regulate sensitivity and dynamic range in *C. elegans* neurons. *Neuron* 20:763–772.
32. Clark DA, Gabel CV, Lee TM, Samuel AD (2007) Short-term adaptation and temporal processing in the cryophilic response of *Caenorhabditis elegans*. *J Neurophysiol* 97:1903–1910.
33. Uchida O, Nakano H, Koga M, Ohshima Y (2003) The *C. elegans che-1* gene encodes a zinc finger transcription factor required for specification of the ASE chemosensory neurons. *Development* 130:1215–1224.
34. Lanjuin A, VanHoven MK, Bargmann CI, Thompson JK, Sengupta P (2003) *Otx/otd* homeobox genes specify distinct sensory neuron identities in *C. elegans*. *Dev Cell* 5:621–633.